Poling-Assisted Fabrication of Plasmonic Nanocomposite Devices in Glass

By *Martynas Beresna, Peter G. Kazansky,* Olivier Deparis, Isabel C. S. Carvalho, Satoshi Takahashi,* and *Anatoly V. Zayats*

Recent advances in nanophotonics and biosensing have been based on the ability to fabricate complex plasmonic nanostructures with enhanced and controllable optical properties.[1–4] Both individual plasmonic nanostructures as well as their arrangements in the so-called metamaterial-type structures have attracted significant attention due to their potential to control light interaction with molecules and various quantum objects, to provide artificial photonic properties for light guiding and manipulation, as well as in high-performance label-free bio- and chemo- sensing based on refractive index sensitivity or the surface-enhanced Raman scattering.[1–4] Majority of such plasmonic nanostructures are fabricated by structuring of thin metal films and surfaces or by various nanoparticles arrangements placed on a surface of a metal or dielectric substrate.

Recently, thermal electric-field poling technique has been developed as an efficient tool for modifying optical and structural properties of glass embedded with noble metal nanoparticles.[5–11] In this article, we demonstrate that this technique can be used for fabrication of plasmonic nanostructures over large surface areas, consisting of an assembly of Au nanoparticles directly inside the glass matrix. This is accompanied also by modification of the refractive index of the glass in the vicinity of the plasmonic nanostructure leading to its unique optical properties. In particular, waveguiding in the plasmonic composite metamaterial layer and anomalous conical light scattering pattern with the enhanced backscattering have been observed which can be used for the development of new types of sensing applications. Exposure of the surface to different kinds of organic vapors leads to significant changes of the backscattering intensity, providing simple way to build an optical bio-, chemical and environmental sensors. The experimental results are supported by numerical modeling of metal-dielectric nanocomposites. The described technique can be used for fabrication of planar as well as patterned plasmonic structures inside glass matrix with the pattern determined solely by the electrode layout.

The initial substrate used for fabrication of plasmonic nanostructures predominantly consists of an electrically conducting soda-lime glass (n_{sub} = 1.488) with a thin electrically resistive sol-gel silicate film (n_{host} = 1.46) on top of it (supplied by Nippon Sheet Glass Co., Japan). The initial sample exhibited pink color due to localized surface plasmon resonance of the Au nanoparticles embedded in glass (**Figure 1c**), which have the extinction peak at around 530 nm wavelength (Figure 1d). The poling process induces change of the optical and physical properties in the region (few microns in thickness) below the anode due to the migration of cations (mainly Na^+ and K^+) in the glass substrate towards the cathode[12, 13] The areas of the sol-gel film which were in the direct contact with the anode became bleached (discoloured) after poling. The bleaching can be explained by electric-field assisted dissolution of gold nanoparticles studied previously.[7] However, since we intentionally avoided complete bleaching of the middle part of the sample, i.e. the film area located below the air gap, gold particles were still present in this area as evidenced by its coloring.

Transmission electron microscopy (TEM) images (Figure 1e) of the sample cross-section in the partially bleached region revealed a 2 μm thick modified layer within the glass substrate, underneath the sol-gel film. This layer is a result of charged carrier migration (e.g. alkali ions in soda lime glass) during the thermal poling process. The modified layer is a part of the region which was depleted of charged carriers and thus, has a higher electrical resistivity than the remaining soda-lime substrate. Many void-like nanoscale features were observed within that layer which were initially absent in the original sample before poling (Figure 1e). The modified layer is expected to have a reduced refractive index (~1.5% less) as compared to the main soda-lime glass substrate.[14]

The diameter of the Au particles in the metal-dielectric composite was estimated from the series of TEM images to be statistically unchanged (~15 nm). This was confirmed by the unchanged position of the extinction resonance (~530 nm) of the poled structure measured at normal incidence. At the same time, the drop in the extinction observed at the resonance, indicated about 20% reduction of the nanoparticle concentration. These observations suggest towards the step-like (explosion-type) dissolution of the Au nanoparticles during poling, rather than their continuous dissolution.[7] Gold clusters, ionized by

[*] M. Beresna, Prof. P. G. Kazansky
Optoelectronics Research Centre
University of Southampton
Southampton SO17 1BJ (UK)
E-mail: pgk@orc.soton.ac.uk
Prof. O. Deparis
Research Centre in Physics of Matter and Radiation (PMR)
University of Namur (FUNDP)
Namur B-5000 (Belgium)
Dr. I. C. S. Carvalho
Pontificia Universidade Católica do Rio de Janeiro
Rio de Janeiro 22453–900 (Brazil)
Dr. S. Takahashi, Prof. A. V. Zayats
Centre for Nanostructured Media
The Queen's University of Belfast
Belfast BT7 1NN (UK)

DOI: 10.1002/adma.201001222

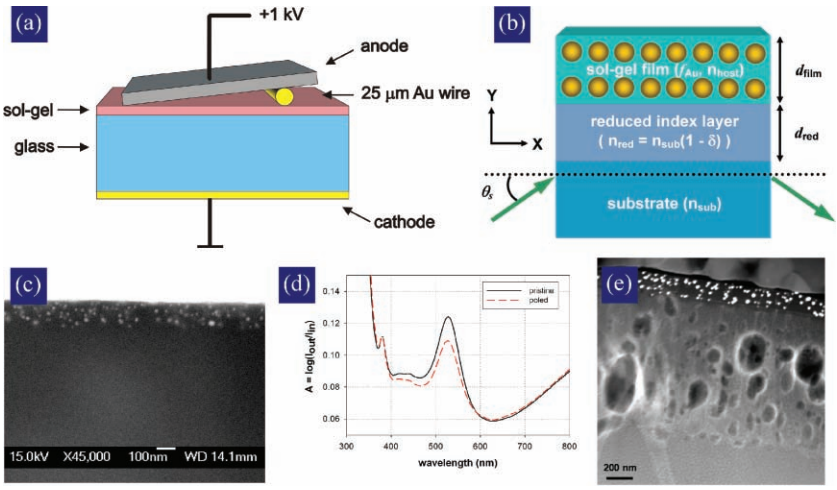

Figure 1. (a) The poling rig arrangement. (b) Schematic of the structure obtained after thermal poling (not to scale). The angle θ_s indicates the angle of incidence. (c) Scanning electron microscopy (SEM) image of the unpoled sample cross-section (image supplied by NSG Co.) showing the 130 nm thick sol-gel film with embedded Au nanoparticles on top of the glass substrate. (d) The extinction spectrum of the pristine and poled samples measured at normal incidence; after poling absorption peak is decreased by about 20% without noticeable shift of the resonance. (e) TEM image of the cross-section of the partially bleached region of the sample after the electric-field thermal poling. The region under the anode reveals the film doped with Au-particles and the modified region of ~2 μm with void like nano-structures in the depletion region.

the escaping electrons, become unstable and "explode" due to the expulsion of gold ions induced by strong Coulomb forces (avalanche process). The remaining cluster becomes neutral again, for a while, but rapidly the ionization starts again and the dissolution process is repeated until the cluster is totally dissolved. The Au nanoparticles remaining after poling have arbitrary spatial arrangement within the layer.

In order to characterizes optical properties of the fabricated nanocomposite metamaterial, reflection and scattering experiments have been performed using a single-mode linearly polarized 10 mW continuous-wave laser operating at λ = 532 nm wavelength close to the plasmonic resonance measured for the structure. We take advantage of the configuration of the fabricated nanocomposite sample (Figure 1b) which resembles the frustrated-total-internal-reflection configuration (Otto configuration) for the studies of surface plasmon polaritons.[15] The soda-lime glass substrate acts as the medium from where light is launched. The reduced refractive index region which was created during thermal poling forms the spacer between the glass and the layer with Au nanoparticles. This layer with smaller refractive index acts as leaky waveguide placed near the plasmonic nanocomposite layer and thus increases interaction length of light with plasmonic nanocomposite.

The angular dependence of the reflectance (**Figure 2a**) clearly exhibits sharp ($\Delta\theta_s$ ~ 1°) resonances for both *s*- and *p*-polarised incident light: θ_s = 11° for *s*-polarization and θ_s = 10.5° for *p*-polarization (θ_s is defined as the angle between the normal to the sample surface and the incident laser beam direction in the X-Y plane of incidence (see Figure 1b)). The leaky waveguiding of the light in the plasmonic composite was clearly observed when excited at these angles through almost the entire region where the Au nanoparticles are present (Figure 2c). At the resonant angles, the reflected intensity was about 0.1 of the nonresonant reflectance, i.e. almost 90% of the incident power was absorbed. (Please note that the total scattered power, as measured in the scattering experiments described below, was approximately 1% of the incident power; therefore, the most of the incident light in the resonance is absorbed in the plasmonic metamaterial). These effects are absent in the unpoled structures (the low-refractive index layer is not present) and in the completely bleached structures (no plasmonic nanocomposite).

To model the observed effects, the reflectance of the 3-layer structure (substrate/depleted region/nanocomposite) was calculated with the plasmonic metamaterial layer described by the effective medium model since both the size of the nanoparticles and the distance between them is much smaller than the wavelength of the light.[15] In the absence of reduced index layer (unpoled sample), the calculated reflectance as a function of the incident angle θ_s reproduces the experimental observations (cf. Figure 2a and b) with the decrease of reflectance with increasing angle and the higher reflection for *p*-polarised light. In the presence of the reduced index layer (poled sample), the resonances due to leaky waveguided modes were observed at specific angles in the simulations, as well as in the experiment. The shape of the reflectance angular spectra is consistent with the experimental results. The closest fit to measurements was achieved for the thickness of the depleted layer of d_{dep} ~ 2 μm, in line with the experimental observations, and the reduction of the refractive index due to poling of δ ~ 1.0%. No other fitting parameters were used.

Under the conditions of the enhanced absorption, peculiar scattering pattern with atypically strong backscattering has been observed from the plasmonic nanocomposite. In the scattering experiments, the sample was fixed on a rotating stage, the same laser source, which was used for reflectance measurements, was shone onto the substrate side surface and focused onto the substrate/film interface within nanocomposite area, at grazing angles of incidence (Figure 1b). An arc-shaped scattering pattern (**Figure 3a**) was clearly observed for the incident angles θ_s ranging from 5° to 13°. The scattering intensity distribution can be described by a surface of a wide-angle cone with stronger scattering in the backward direction. (The arc observed on the screen in Figure 3a is a part of a ring that constituted the base of a cone.) By rotating the sample, i.e. by changing θ_s, the highest intensity of backscattering was observed at θ_s ~ 11° for *s*-polarization and at θ_s ~ 10.5° for *p*-polarization of the incident light. These are the same angles at which the excitation of the waveguided mode and minimum of the reflectance were observed (Figure 2). As was noted above, the total scattered power was approximately 1% of the incident power. Thus, the reduction of the reflection is not at the expense of the increased scattering but rather increased absorption. In the similar way, as increased transmission of the plasmonic crystals

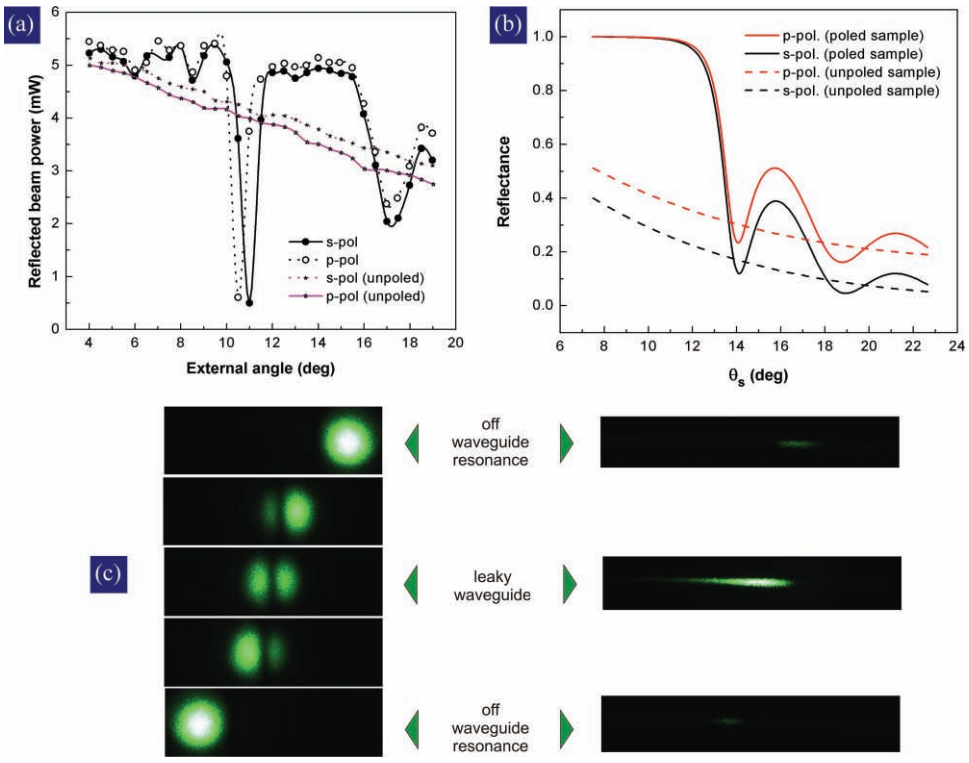

Figure 2. (a) Angular dependence of the reflectance of the unpoled and poled samples for *s*- and *p*-polarization of the incident light. The resonant absorption occurs at $\theta_s = 11°$ for *s*-polarization (solid line) and $\theta_s = 10.5°$ for *p*-polarization (dotted line) when the waveguided mode is excited. (b) Effective medium simulations of the reflectance of poled (solid lines) and unpoled (dashed lines) samples for *s*- and *p*-polarized light (black and red lines, respectively). (c) (LEFT) The images of the reflected beam in the far-field at the resonant and non-resonant angles of incidence for *s*-polarization of the incident light and (RIGHT) the corresponding images taken near the point of incidence of the beam at the substrate—film interface.

is accompanied by the reduced reflection and the increased absorption.[16,17]

The observed angular scattering diagram (Figure 3b) exhibits pronounced forward and backward scattering lobs. When the beam was *s(p)*-polarized, vanishing (maximum) scattering power intensity was observed at a scattering angle of 90° with respect to the incident beam direction. At the same time, when the laser beam was focused onto the completely bleached areas of the sample (no plasmonic nanocomposite), the scattered power decreased drastically with isotropic scattering pattern. The conical scattering was also absent for other samples tested that were fabricated with different poling parameters and arrangements[6] but all completely bleached (no metal nanoparticles).

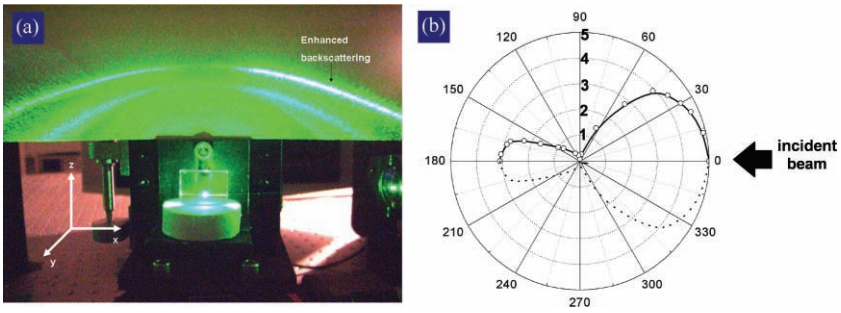

Figure 3. (a) True image of the anomalous conical scattering pattern with stronger backscattering for an *s*-polarized light incident at $\theta_s = 11°$ (the laser beam is traveling from right to left). The observation screen was placed at a distance of 10 cm from the sample parallel to the substrate surface. (b) Polar representation of scattered optical power distribution at the base of the cone under the same illumination conditions as in (a); forward and backward scattering directions correspond to 180° and 0° polar angles, respectively. Bottom part is symmetrically drawn for eye guidance.

To model the observed phenomenon of backscattering in Rayleigh regime, the reflectance and scattering properties of the sample were studied numerically using the 3D transfer matrix method.[18] (Please note that since multiple scattering effects are important, it cannot be modeled in the effective medium approximation regime describe above). The glass substrate was assumed to be semi-infinite. The region of the substrate which was modified by poling was treated as a homogeneous layer with reduced refractive index. The nanocomposite film was considered as 8 layers of thickness equal to the experimentally estimated gold particle diameter $b = 15$ nm and random distribution of several (N) gold spheres within each layer. The filling factor was set similar to the experimentally determined by taking $N = 8$ spheres in the unit cell ($f_{Au} = 2.48\%$).

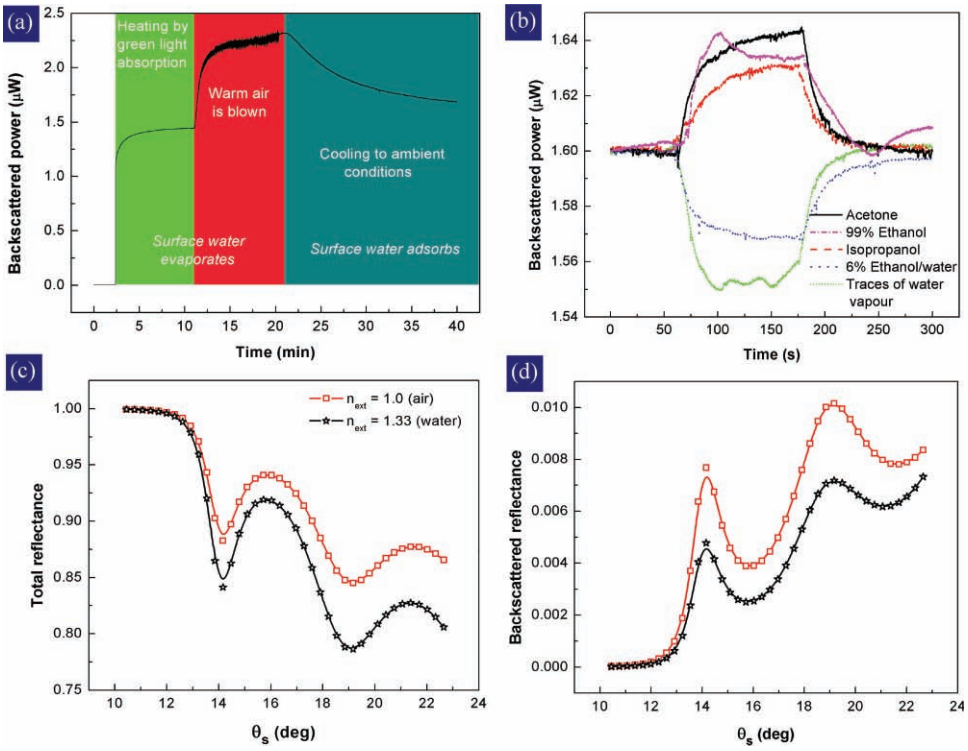

Figure 4. (a) Variations of the backscattering when the sample is flashed with warm (35 °C) dry air. (b) Variations of the backscattering when the sample is exposed to various vapors at the interval around 60–160 s. (c,d) Numerical simulations of total and backscattered reflectance of the poled sample for two different superstrate media: air (squares) and water (stars).

Due to randomness in the spheres positions, the scattering quantities became statistical quantities and were computed for 10 different statistical realizations of the nanoparticle arrangement (**Figure 4d**). The total reflectance spectrum was found to be almost identical to the case of periodically arranged particles and, in turn, in a good agreement with effective medium calculations (Figure 2d) and only weakly depends on the statistical distribution, as it should be expected. The backscattering intensity, on the other hand, was found to be strongly dependent on the particle spatial arrangement as it is significantly influenced by the multiple scattering effects on the spheres. Stronger backscattering is predicted for clustered nanoparticles (see Supporting Material). Again, the model predicts correctly the position of the resonance angle at which strongest scattering has been observed, which corresponds to the reflection minimum.

As was analyzed from the TEM images (Figure 1d) of the nanocomposites, the gold spheres are stochastically distributed within the layer. Some of them form clusters of 2 or 3 particles and it seems that there is also an overall interspacing of on average 200 nm between some particles, which is close to spatial period yielding optimal backscattering in the modeling. Therefore, only a small fraction of the particles form a more or less regular lattice with 200 nm spacing, which produces the backscattering. The rest of the particles are randomly distributed (with aggregations) and contribute to incoherent scattering background on top of which the backscattering is observed.

It is well known that plasmonic nanostructures and metamaterials are very sensitive to the refraction index of the surrounding medium and often used for label-free sensing applications.[1,2] In many cases complex experimental configurations are required to access the resonant conditions of surface plasmon excitation. Remarkably, the observed backscattering, being intrinsically determined by the interaction within plasmonic layer also possesses strong sensitivity to the refractive index of the substance above the nanocomposite layer and can be used for sensing application in the simple arrangements where only the detection of the scattering intensity is required.

Sensing properties of the structure can be described within the same model as above, considering different superstrates (air: $n_{ext} = 1$ and water: $n_{ext} = 1.33$) above the nanocomposite layer (Figure 4d). One can readily see that the increase of the refractive index reduces both scattered and reflected signals. At the same time, the position of the observed resonances does not depend on the superstrate. The origin of the effect is in the modification of the waveguided mode excited in the nanocomposite layer. Interestingly, backscattering is much more sensitive to ambient environment than the reflection (cf. Figure 4c and 4d).

In order to experimentally demonstrate the effect, we studied the effect of the water removal from the nanocomposite layer (Figure 4a). The backscattering power was monitored while exposing the sample to the stream of dry air. When the laser is switched on in the ambient conditions, the scattering increases due to the heating of the sample related to the laser light absorption in the nanoparticles and related water molecule desorption. When the sample is heated to 35 °C in the dry atmosphere environment, the backscattered power sharply rises by about

60% within first 20 s of the exposure followed by saturation at the end of 10 min with almost 70% increase of the backscattered power. When the sample is again exposed to initial ambient conditions, the scattered power steadily decreased back to the initial value in an exponential fashion due to adsorption of water molecules from the atmosphere. Numerous studies of the adsorption on glass surface suggest that even in the driest of environments, glass samples have a layer of adsorbed water ranging from a few angstroms to several nanometers depending on the relative humidity.[19,20] Another possible effect may also be associated with water molecules from the ambient environment penetrating into porous sol-gel matrix.[7,21]

To further illustrate this effect, the sample, originally in the ambient conditions, was exposed to organic vapors (ethanol, 2-propanol, methanol, acetone) that are known to contribute to drying the glass surface via removing molecular layers of water existing on the surface. An appreciable increase in the backscattered power was observed when the surface is contact with those vapors (Figure 4b). At the same time, when the sample is exposed to vapors containing traces of water molecules, the backscattered intensity decreases due to water molecule adsorption on the surface. In parallel, with the changes in the backscattering under the vapor exposure, there was also observed a proportional change in the reflectance of the sample, but with much smaller relative variations and thus requiring more cumbersome detection. Hence, this system, after precise calibration, could potentially be used for sensing organic vapors and humidity.

In summary, electric-field assisted poling has been demonstrated as efficient and inexpensive tool for fabrication of plasmonic metamaterials (metal-dielectric nanocomposites) directly within glass substrate over large areas. The refractive index modification of the host medium near the plasmonic structure during fabrication results in the formation of the plasmonic metamaterial with peculiar optical properties, enabling excitation of leaky waveguided modes in the composite layer as well as leading to the enhanced backscattering effects. The concept of the enhanced interaction of light with gold nanocomposites can be exploited for developing novel bio-, chemical and environmental sensors and other nanophotonics applications. We have demonstrated that the exposure of the sample surface to different kinds of organic vapors leads to a rapid substance-dependent change in the backscattered intensity which can be detected by simple illumination of the sample with a laser beam without any special arrangements.

Acknowledgements

We would like to thank K. Sakaguchi, Y. Ichinomiya and V. Serikov from Nippon Sheet Glass for the help and support of this project. Also authors are grateful to C. Corbari for valuable comments.

Received: April 4, 2010
Revised: May 5, 2010
Published online: July 22, 2010

[1] J. N. Anker, W. P. Hall, O. Lyandres, N. C. Shah, J. Zhao, R. P. Van Duyne, *Nat. Mater.* **2008**, *7*, 442.
[2] S. Lal, S. Link, N. J. Halas, *Nat. Photonics* **2007**, *1*, 641.
[3] W. L. Barnes, A. Dereux, T. W. Ebbesen, *Nature* **2003**, *424*, 824.
[4] T. W. Ebbesen, C. Genet, S. I. Bozhevolnyi, *Phys. Today* **2008**, *61*, 44.
[5] O. Deparis, P. G. Kazansky, A. Abdolvand, A. Podlipensky, G. Seifert, H. Graener, *Appl. Phys. Lett.* **2004**, *85*, 872.
[6] O. Deparis, P. G. Kazansky, A. Podlipensky, A. Abdolvand, G. Seifert, H. Graener, *J. Appl. Phys.* **2006**, *100*, 044318.
[7] F. P. Mezzapesa, I. C. S. Carvalho, P. G. Kazansky, O. Deparis, M. Kawazu, K. Sakaguchi, *Appl. Phys. Lett.* **2006**, *89*, 183121.
[8] A. Abdolvand, A. Podlipensky, S. Matthias, F. Syrowatka, U. Gosele, G. Seifert, H. Graener, *Adv. Mat.* **2005**, *17*, 2983.
[9] A. A. Lipovskii, M. Kuittinen, P. Karvinen, K. Leinonen, V. G. Melehin, V. V. Zhurikhina, Yu. P. Svirko, *Nanotechnology* **2008**, *19*, 415304.
[10] J. Sancho-Parramon, V. Janicki, J. Arbiol, H. Zorc, F. Peiro, *Appl. Phys. Lett.* **2008**, *92*, 163108.
[11] Z. Zou, X. Chen, Q. Wang, S. Qu, X. Wang, *J. Appl. Phys.* **2008**, *104*, 113113.
[12] R. A. Myers, N. Mukherjee, S. R. J. Brueck, *Opt. Lett.* **1991**, *16*, 1732.
[13] P. G. Kazansky, P. S. Russell, *Optics Commun.* **1994**, *110*, 611.
[14] W. Margulis, F. Laurell, *Appl. Phys. Lett.* **1997**, *71*, 2418.
[15] A. Otto, *Z. Phys.* **1968**, *216*, 398.
[16] D. Gerard, L. Salomon, F. de Fornel, A. V. Zayats, *Phys. Rev. B*, **2004**, *69*, 113405.
[17] D. Gerard, L. Salomon, F. de Fornel, A. V. Zayats, *Opt. Express*, **2006**, *12*, 3652.
[18] J. P. Vigneron, V. Lousse, in *Photonic Crystal Materials and Devices IV*, Vol. *6128* (Eds. A. Adibi, S. Y. Lin, A. Scherer), Spie-Int Soc Optical Engineering, Bellingham **2006**; pp G1281–G1281.
[19] J. Freund, J. Halbritter, J. H. H. Horber, *Microsc. Res. Tech.* **1999**, *44*, 327.
[20] K. Tiefenthaler, W. Lukosz, *Opt. Lett.* **1984**, *10*, 137.
[21] L. N. Xu, J. C. Fanguy, K. Soni, S. Q. Tao, *Opt. Lett.* **2004**, *29*, 1191.